Appendix: For Online Publication

Contents

A Data for the empirical analysis and an additional motivating fact

I use the U.S. Compustat data for firm-level empirical analyses. Firms with negative assets and zero employment are excluded from the sample. All firm-level variables except capital stock and investment are deflated by the GDP deflator. Investment is deflated by non-residential fixed investment deflator available from National Income and Product Accounts data (NIPA Table 1.1.9, line 9). The firm-level real capital stock is obtained by applying the perpetual inventory method to deflated net investment. The net investment is obtained from the lag difference of the balance sheet item Property, Plant, and Equipment (Net). The capital stock therefore includes only tangible assets and excludes intangible capital. The industry is categorized by the first two-digit NAICS code.[1]

A.1 Conditional heteroskedasticity

Figure A.1: Conditional heteroskedasticity of aggregate investment

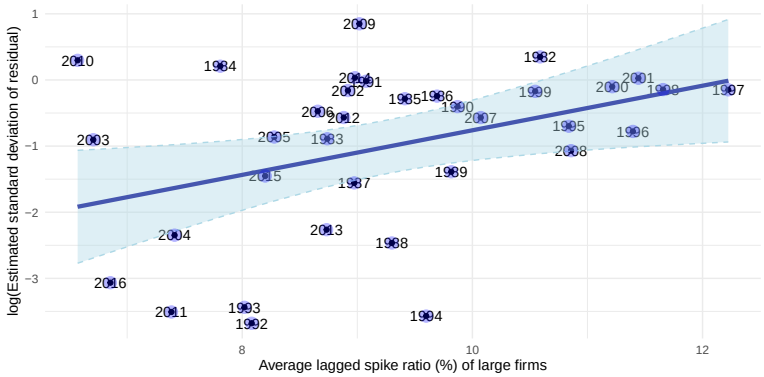

Notes: The estimated standard deviation of the residual (y-axis) is obtained from fitting the aggregate investment-to-capital ratio (%) into an autoregressive process with four lags. The average lagged spike ratio of large firms (%) is obtained by averaging the most recent past two spike ratios for each observation of residualized investments. The years overlaid on the dots are the observed years of the residualized investment-to-capital ratios.

I show aggregate investment rate is conditionally heteroskedastic on the average lagged

[1] If only SIC code is available for a firm, I imputed the NAICS code following online appendix D.2 of Autor et al. (2020). If both NAICS and SIC are missing, I filled in the next available industry code for the firm.

spike ratio of large firms. That is, the residualized volatility of aggregate investment rate is high if a great portion of large firms have recently made lumpy investments synchronously.

For this analysis, I use aggregate data on non-residential investment (NIPA Table 1.1.5, line 9) and aggregate capital (Fixed Asset Accounts Table 1.1, line 4) from BEA. The thick line in Figure A.1 plots the estimates of the log standard deviation of residuals from the autoregression of aggregate investment rates as a function of the recent average of large firms' spike ratio.[2] The recent average is based on the average spike ratio of the past two years. As can be seen from this figure, aggregate investment rates are heteroskedastic conditional on the lagged average spike ratio. Table A.1 reports the regression coefficients for the fitted line. According to the regression result, a one-standard-deviation increase (1.47%) in the large firms' past spike ratio is associated with a one-standard-deviation increase (0.50%) in the aggregate investment's residualized volatility. Consistent with the patterns in Figure 1 in the main text, the three recession years of interest are located at the top-right corner in Figure A.1.

Table A.1: Residual volatility of the aggregate investment and spike ratios

	Dependent variable: $log(\hat{\sigma}_t)$	
	Large	Small
$\overline{spike}_{t-1}$ (%)	0.337	0.077
	(0.138)	(0.074)
Constant	−4.131	−2.317
	(1.290)	(1.270)
Observations	35	35
R^2	0.154	0.032
Adjusted R^2	0.128	0.002

Notes: The dependent variable is the log absolute value of the residuals from fitting the aggregate investment to capital ratio into AR(4) process. The independent variables are the past average spike ratio, $\overline{spike}_{t-1}$, and the intercept.

[2]This empirical analysis is motivated from the conditional heteroskedasticity analysis in Figure 1 of Bachmann et al. (2013). Differently from theirs, the focus is on the large firms' recent lumpy investments.

The independent variable $\overline{spike}_{t-1}$ is defined as follows:

$$\overline{spike}_{t-1} := \frac{1}{J}\sum_{j=0}^{J-1} SpikeRatio_{t-1-j}$$

$$SpikeRatio_t := \frac{\#\text{Extensive-margin adjustment}_t}{\#\text{Firms}_t}$$

where J is the number of past years to be included in the average. In the reported result, I use $J = 3$. The result is robust over $J = 1, 2, 4$.

B Firm-level interest elasticity in the models and the data

B.1 Firm-level interest elasticities of investments in the models

This section compares the semi-elasticities of firm-level investment across different models. I compare six different models: 1) a baseline model with $\zeta = 3.7$; 2) calibrated baseline model ($\zeta = 3.5$); 3) a baseline model with $\zeta = 2$; 4) a baseline model with $\zeta = 0$ (Winberry, 2021); 5) a model with only convex adjustment cost (no fixed cost); and 6) a model with only fixed adjustment cost (no convex adjustment cost) (Khan and Thomas, 2008). The models are calibrated to match the same calibration targets as the calibrated baseline model in the main text except for the cross-sectional semi-elasticities.[3] Additionally, for the model with both fixed and convex adjustment costs, I matched the cross-sectional dispersion of the investment-to-capital ratio.

Table B.2 reports the semi-elasticities of firm-level investments for different groups across different models. The elasticities are measured by the average contemporaneous change in the firm-level investment in per cent from the steady-state when the interest rate changes by 1%.[4] In particular, I calculate the average between the elasticity measured when the interest rate increases by 1% and the one measured when the interest rate decreases by 1% to address the asymmetry in the responses to the positive and negative interest rate shocks.

[3] The target moment is the same as in the baseline model calibration, which is reported in Table 3 of the main text.

[4] The elasticity is measured in the partial equilibrium as in Winberry (2021) and Koby and Wolf (2020).

The average interest-elasticity of group $j \in \{All, Small, Large\}$ is defined as follows:

$$Elasticity_{jt} = \frac{\int_{\{I_{ijt}>0\}} \Delta log(I_{ijt}\psi_{ijt} + I^c_{ijt}(1-\psi_{ijt}))d\Phi_j}{\Delta r_t}$$

where ψ_{ijt} is the extensive-margin adjustment probability; I_{ijt} is then investment after fixed cost is paid and I^c_{ijt} is the investment when the fixed cost is unpaid; Φ_j is the joint distribution of firms conditional on group j.

The extensive-margin elasticity of group $j \in \{All, Small, Large\}$ is defined as the average contemporaneous change in the firm-level investment driven by extensive-margin probability changes in per cent from the steady-state when the interest rate changes by 1%. Therefore, the investment policy functions are fixed at the steady-state level, while the extensive-margin probabilities deviate from the steady-state:

$$Elasticity^{ext}_{jt} = \frac{\int_{\{I_{ijt}>0\}} \Delta log(I^{ss}_{ijt}\psi_{ijt} + I^{ss,c}_{ijt}(1-\psi_{ijt}))d\Phi_j}{\Delta r_t}$$

where ψ_{ijt} is the extensive-margin adjustment probability; I_{ijt} is then investment after fixed cost is paid and I^c_{ijt} is the investment when the fixed cost is unpaid; Φ_j is the joint distribution of firms conditional on group j.

The intensive-margin elasticity of group j is defined as the average contemporaneous change in the firm-level investment driven by investment magnitude changes in per cent from the steady-state when the interest rate changes by 1%. Therefore, the extensive-margin probability is fixed at the steady-state level, while the investment policy functions deviate from the steady-state.

$$Elasticity^{int}_{jt} = \frac{\int_{\{I_{ijt}>0\}} \Delta log(I_{ijt}\psi^{ss}_{ijt} + I^c_{ijt}(1-\psi^{ss}_{ijt}))d\Phi_j}{\Delta r_t}.$$

The elasticity of the spike ratio of group j is defined as the average contemporaneous change in the fraction of firms investing greater than 20% of the existing capital stock when

the interest rate changes by 1%.

$$Elasticity_{jt}^{SpikeRatio} = \frac{\int_{\{I_{ijt}>0\}} \Delta \mathbb{I}\left\{\frac{I_{ijt}\psi_{ijt}+I_{ijt}^{c}(1-\psi_{ijt})}{k_{ijt}} > 0.2\right\} d\Phi_j}{\Delta r_t}$$

In Table B.2, the first four rows of the table report the elasticities of investment conditional on $I_{ijt} > 0$ where i is a firm index, j is a size group indicator, and t is the time subscript; the next four rows report the extensive-margin elasticities; the following four rows report the intensive-margin elasticities; the last four rows report the spike ratio elasticities.[5] The elasticity of investment is as defined in section B.1. I calculate the average between the elasticity measured when the interest rate increases by 1% and the one measured when the interest rate decreases by 1% to address the asymmetry in the responses to the positive and negative interest rate shocks.

As can be seen from the columns other than the second and the third in Table B.2, the aggregate investment elasticities are well-matched with the empirical level once both convex and fixed adjustment costs are considered. Especially, the inclusion of convex adjustment cost dramatically dampens the aggregate elasticity, as can be seen from the aggregate elasticity in the fifth column compared to that of the sixth column (Winberry, 2021; Koby and Wolf, 2020).

The cross-sectional elasticity ratio between small and large in other models than the baseline cannot match the empirical estimate of 1.95 from Zwick and Mahon (2017). As the fixed cost becomes size-dependent and as the intra-firm interdependence across establishments rises, the cross-sectional elasticity ratio increases. From the middle and lower part of the table, the size-dependence and the intra-firm linkages increase not only the extensive-margin S/L ratio but the intensive-margin S/L ratio. This is due to the selection effect on those large firms that remain to adjust despite the higher fixed cost.

Sensitivity and monotonicity The cross-sectional semi-elasticity ratio between small and large firms smoothly and monotonically increase in the parameter ζ. These results

[5] Following Zwick and Mahon (2017), I define the elasticity conditional on $I_{ijt} > 0$ as investment elasticity.

Table B.2: Semi-elasticity of investment across the models and the decomposition

	$\zeta = 3.7$	$\zeta = 3.5$ (baseline)	$\zeta = 2$	$\zeta = 0$	convex only	fixed only
Investment						
All	6.52	6.6	6	6.4	5.85	256.80
Small	9.13	8.93	6.55	4.9	5.62	179.54
Large	3.98	4.92	4.67	10.06	6.82	403.02
S/L ratio	2.29	1.81	1.4	0.49	0.82	0.45
Ext. margin						
All	3.47	3.44	3.19	3	3.09	68.38
Small	4.96	4.91	4.22	3.27	3.75	79.14
Large	1.95	1.97	2.18	2.68	2.41	63.42
S/L ratio	2.54	2.49	1.94	1.22	1.56	1.25
Int. margin						
All	3.04	3.15	2.8	3.4	2.76	72.59
Small	4.14	4	2.32	1.62	1.86	62.61
Large	2.03	2.95	2.49	7.38	4.4	90.43
S/L ratio	2.04	1.36	0.93	0.22	0.42	0.69
Spike ratio						
All	1.45	1.46	1.21	1.46	1.28	22.09
Small	2.82	2.82	1.85	2.92	1.56	27.95
Large	0.42	0.49	0.41	0.73	0.6	13.35
S/L ratio	6.71	5.76	4.45	4.02	2.58	2.09

Notes: The semi-elasticities of investment variables are computed from the contemporaneous response to an interest rate change in the partial equilibrium. To address the asymmetry between responses to the positive and negative interest rate shocks, I report the average responses to the positive 1% and negative 1% interest rate changes.

demonstrate two key points: (1) the parameter ζ is indeed critical for generating both the correct elasticity patterns and the fragility mechanism, and (2) the results vary smoothly with ζ, indicating that my findings are not driven by a knife-edge parameter choice. The baseline value of $\zeta = 3.5$ emerges naturally from matching the empirical elasticity patterns.

B.1.1 Elasticity visualization

Figure B.2 visualizes the large and small firms' interest elasticities for the baseline model (panel (a)), for a model with fixed cost only (panel (b)), and for a model with $\zeta = 0$ (panel (c)).[6] Throughout this paper, all the alternative models to the baseline are calibrated to sharply match the target moments except for the cross-sectional semi-elasticity ratio.

[6]The model with convex and fixed adjustment cost is a prototype of the models in Winberry (2021) and Koby and Wolf (2020).

Figure B.2: Semi-elasticities of investments across different models

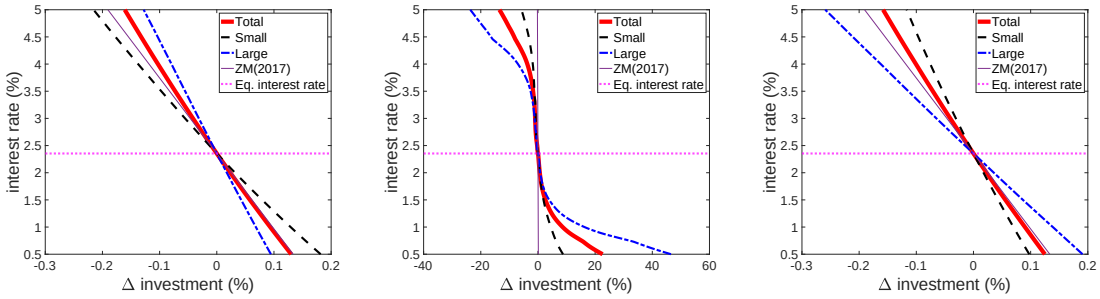

(a) Baseline ($\zeta = 3.5$) (b) Fixed only (c) Convex + Fixed ($\zeta = 0$)

Notes: The figure plots the deviation of investment from the steady-state level when the interest rate changes for each different model. The vertical axis is the interest rate in per cent, and the horizontal axis is the percentage deviation from the steady-state investment. The horizontal dotted line indicates the equilibrium interest rate. The thin solid line labeled as ZM (2017) indicates Zwick and Mahon (2017)'s reference level of 7.5.

In each panel, the vertical axis is the interest rate in per cent, and the horizontal axis is the percentage deviation from the steady-state investment. The horizontal dotted line indicates the equilibrium interest rate. As the interest rate decreases, all models' average deviation of investment from the steady-state increases. In the baseline model (panel (a)), the ranking of the interest elasticity across the firm-size group is consistent with the empirical patterns, as can be seen from the steeper curve of the large firms. However, in the model with $\zeta = 0$ (panel (c)), the large firms' average deviation of investment from the steady-state increases faster than small firms as the interest rate decreases. In the model with a fixed cost only (panel (b)), the interest elasticities of all groups are significantly higher than the ones in the other two models, as can be checked from the large-scale variation along the horizontal axis.

B.2 Firm-level interest-elasticities of investments in the data

In this section, I empirically estimate the elasticity of firm-level investment using firm-level balance sheet data and monetary policy shocks in the literature. Prior research papers in the literature have provided the well-identified interest-elasticities of firm-level investments, but those estimates are not informative enough to pin down the missing component in the existing model frameworks. For this, I estimate the elasticities of small and large firms' spike ratios to develop a model with realistic firm-level investment.

I estimate the following regression separately for large firms and small firms:

$$f(k_{it}, k_{it+1}) = \beta MP_t + \alpha_i + \alpha_{sy} + Controls_{it} + \epsilon_{it}$$

where MP_t is the monetary policy shock; α_i is firm fixed effect; α_{sy} is sector-year fixed effect. The control variables include lagged current account (ACT_{t-1}), lagged total debt (DT_{t-1}), and operating profit ($OIBDP_t$) normalized by lagged total asset (AT_{t-1}), log of lagged capital stock, and log of employment (EMP_t). The standard errors are two-way clustered across firms and years.

Table B.3 reports the coefficient of monetary policy shock (MP_t) for large and small firms across different choices of dependent variables.[7] As can be seen from the first two columns, the elasticity of the investment is significantly lower in large firms than in small firms. This is consistent with the empirical results in the literature and contradictory to the model-implied elasticities in the previous section. Also, the sensitivity of the spike ratio is significantly lower in large firms than small firms, as reported in the third and fourth columns.[8]

The differences in the elasticities in Table B.2 and Table B.3 sharply indicate that the existing models with fixed and convex adjustment costs cannot correctly capture the ranking of interest-elasticities between large and small firms. Therefore, a new model is needed to study the role of large firms' investments over the business cycle. Then, a question still

[7] I check the robustness of result using a different cutoff 10% than 20% in Table B.4.

[8] Two estimates are statistically different under the significance level of 0.05.

Table B.3: Investment sensitivities to the monetary policy shocks

	Dependent variables:			
	$log(I_{it})$		$\mathbb{I}\{\frac{I_{it}}{k_{it}} > 0.2\}$	
	L	S	L	S
MP_t	-2.201	-7.025	-0.870	-2.072
	(0.606)	(2.41)	(0.367)	(0.676)
Obs.	29,400	7,903	29,400	7,903
R^2	0.929	0.791	0.603	0.558
Firm FE	Yes	Yes	Yes	Yes
Sect.-year FE	Yes	Yes	Yes	Yes
Firm-level ctrl.	Yes	Yes	Yes	Yes
Two-way cl.	Yes	Yes	Yes	Yes

Notes: The independent variables include monetary policy shocks, fixed effects (firm and sector-year), and firm-level control variables (lagged current account (ACT_{t-1}), lagged total debt (DT_{t-1}), and operating profit ($OIBDP_t$) normalized by lagged total asset (AT_{t-1}), log of lagged capital stock, and log of employment (EMP_t)). The numbers in the bracket are the standard errors. The standard errors are clustered two-way by firm and year.

remains about which component of the existing model needs to be improved to capture the empirical relationship. There are broadly two options: lowering either intensive or extensive margin elasticities of large firms.

On this issue, the elasticity of spike ratio gives an answer. I set the model with both fixed and convex adjustment costs as a benchmark model. From the comparison of the interest-elasticities of spike ratios between the benchmark model and the data, the large firms' spike ratio needs to be less elastic, and small firms' spike ratio needs to be more elastic than in the benchmark model to match the empirical counterpart. Therefore, the extensive-margin elasticity needs to be improved from the benchmark model. In the following section, I develop a heterogeneous-firm real business cycle model where the elasticities of investments and spike ratios are at the empirically-supported level through the modification in the extensive-margin investment patterns of the benchmark model.

In the following tables, I report a set of extended regression results using the tight (Table B.4) and wide (Table B.5) window monetary policy shocks.

Table B.4: Investment sensitivity to the monetary policy shocks with the narrow window

	Dependent variables:									
	$log(I_{it})$		$\mathbb{I}\{\frac{I_{it}}{k_{it}} > 0.1\}$		$\mathbb{I}\{\frac{I_{it}}{k_{it}} > 0.2\}$		$log(I_{it}) \mid_{\frac{I_{it}}{k_{it}}>0.1}$		$log(I_{it}) \mid_{\frac{I_{it}}{k_{it}}>0.2}$	
	L	S	L	S	L	S	L	S	L	S
$MP_{Tight,t}$	-2.201	-7.025	-0.656	-2.993	-0.870	-2.072	-0.936	-2.317	-0.246	-3.512
	(0.606)	(2.41)	(0.363)	(0.688)	(0.367)	(0.676)	(0.676)	(1.668)	(0.912)	(2.188)
Obs.	29,400	7,903	29,400	7,903	29,400	7,903	19,524	5,039	11,181	3,643
R^2	0.929	0.791	0.596	0.562	0.603	0.558	0.954	0.865	0.96	0.895
Firm FE	Yes	Yes	Yes	Yes	Yes	Yes	Yes	Yes	Yes	Yes
Sect.-year FE	Yes	Yes	Yes	Yes	Yes	Yes	Yes	Yes	Yes	Yes
Firm-level ctrl.	Yes	Yes	Yes	Yes	Yes	Yes	Yes	Yes	Yes	Yes
Two-way cl.	Yes	Yes	Yes	Yes	Yes	Yes	Yes	Yes	Yes	Yes

Notes: The dependent variable of the probit regression is the indicator of lumpy investment. The independent variables include monetary policy shocks, fixed effects (sector, year, and sector-year), and firm-level control variables (lagged total debt (DT), lagged current account (ACT), lagged size (AT), and sales (Sale) growth). The numbers in the bracket are the standard errors. The standard errors are clustered two-way by sector and year.

Table B.5: Investment sensitivity to the monetary policy shocks with the wide window

	Dependent variables:									
	$log(I_{it})$		$\mathbb{I}\{\frac{I_{it}}{k_{it}} > 0.1\}$		$\mathbb{I}\{\frac{I_{it}}{k_{it}} > 0.2\}$		$log(I_{it}) \mid_{\frac{I_{it}}{k_{it}}>0.1}$		$log(I_{it}) \mid_{\frac{I_{it}}{k_{it}}>0.2}$	
	L	S	L	S	L	S	L	S	L	S
$MP_{Wide,t}$	-2.178	-6.583	-0.643	-2.856	-0.762	-1.870	-0.850	-1.703	-0.333	-3.400
	(0.662)	(2.604)	(0.383)	(0.73)	(0.377)	(0.728)	(0.698)	(1.835)	(0.956)	(2.44)
Obs.	29,400	7,903	29,400	7,903	29,400	7,903	19,524	5,039	11,181	3,643
R^2	0.929	0.791	0.596	0.562	0.603	0.558	0.954	0.865	0.96	0.895
Firm FE	Yes	Yes	Yes	Yes	Yes	Yes	Yes	Yes	Yes	Yes
Sect.-year FE	Yes	Yes	Yes	Yes	Yes	Yes	Yes	Yes	Yes	Yes
Firm-level ctrl.	Yes	Yes	Yes	Yes	Yes	Yes	Yes	Yes	Yes	Yes
Two-way cl.	Yes	Yes	Yes	Yes	Yes	Yes	Yes	Yes	Yes	Yes

Notes: The dependent variable of the probit regression is the indicator of lumpy investment. The independent variables include monetary policy shocks, fixed effects (sector, year, and sector-year), and firm-level control variables (lagged total debt (DT), lagged current account (ACT), lagged size (AT), and sales (Sale) growth). The numbers in the bracket are the standard errors. The standard errors are clustered two-way by sector and year.

C Empirical validation: spike ratio dynamics in model vs. data

In this section, I validate the calibrated baseline model by comparing model-implied large firm spike ratios with their observed counterparts from Compustat using actual TFP series. The global solution method recovers the full dynamics of recursive competitive equilibrium (RCE) allocations over the state space realized along the equilibrium path. Therefore, given the initial endogenous state (or sufficient statistic) and the stream of exogenous state realizations, the corresponding equilibrium path can be computed.[9]

Figure C.3 plots the time series of spike ratios in the model (solid line) and the data (dashed line). For the exogenous TFP series, I use the TFP from the Bureau of Labor Statistics (BLS) (panel (a)) and from Fernald (2014) (panel (b)). The initial state is determined by the level that maximizes the fit (mean-squared distance) between the model and data spike ratio series.

Figure C.3: Model-implied vs. observed spike ratios using actual TFP series

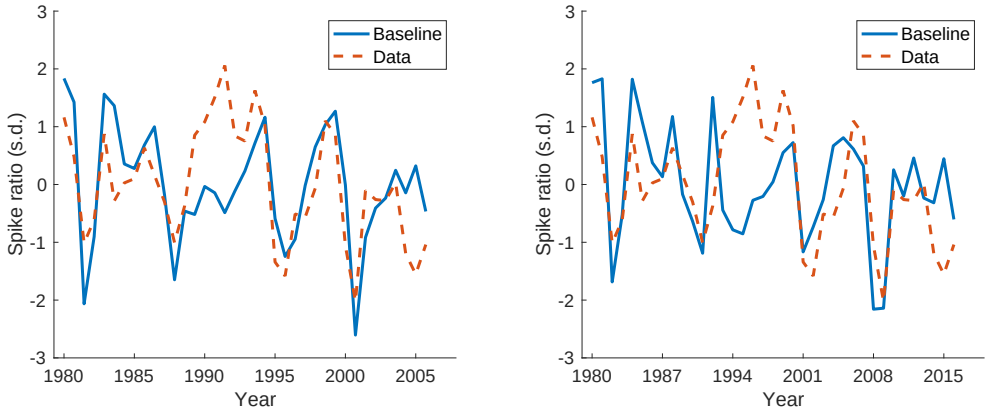

(a) BLS (b) Fernald (2014)

Notes: Figure plots the time series of spike ratios in the model (solid line) and the data (dashed line). The TFP series for the baseline model in panel (a) is from the Bureau of Labor Statistics (BLS), and the TFP data for panel (b) is from Fernald (2014).

[9]The exact combination of endogenous and exogenous states may not be available in the simulated equilibrium path. Therefore, I use the two-dimensional interpolation to obtain policy functions using the nearest state realizations.

As shown in Figure C.3, the spike ratios in the model and data follow closely related patterns, which validates the calibrated baseline model. One noticeable divergence occurs just before the dot-com crash, when the data exhibit a stronger surge in spikes, likely reflecting sector-specific dynamics outside the model's scope. The time series of panel (a) features correlation of 0.58 for the full time series and 0.79 without the prior 7 years before the dot-com bubble crash (30 observations), which are all statistically significant at the 5% significance level. For panel (b), the correlation coefficient is 0.46 for the full series and 0.72 without the prior 7 years before the dot-com bubble crash (30 observations) at the 5% significance level.

D Monetary policy shock

I construct an exogenous monetary policy shock following Ottonello and Winberry (2020) and Jeenas (2018). The monetary policy shock is obtained by time aggregating high-frequency monetary policy shock identified from the unexpected jump (drop) in the federal funds rate during a 30-minutes window around the FOMC announcement.[10] To capture the unexpected component in the federal funds rate, I use the change in the rate implied by the current-month federal funds futures contract. All the data on the timings of the FOMC announcement and the high-frequency surprise are from Gurkaynak et al. (2005) and Gorodnichenko and Weber (2016). The sample period covers from March 1990 until December 2009. I follow the convention that the positive monetary policy shock is an unexpected increase in the federal funds futures rate, so it implies the contractionary monetary policy.

To match the data frequency between the firm-level data and the monetary policy shock, I time aggregate the monetary policy shocks. Specifically, I compute the one-year backward weighted average monetary policy shock at each firm's financial year end. The weight of each surprise is determined by the number of days between the corresponding FOMC announcement and the next FOMC announcement.[11] If the next FOMC announcement was made after the financial year end, the days are counted until the financial year end. This data joining process matches a firm's balance sheet information and the monetary policy shock at the same financial year. The weighted moving average monetary policy shock is plotted in Figure D.4.

[10] The result is robust over the choice of a wider window (one-hour window) as reported in Table B.5.

[11] A higher weight is assigned for a monetary policy shock when there was greater amount of time for a firm to respond to the shock (Ottonello and Winberry, 2020).

Figure D.4: One-year moving average monetary policy shock: March 1990 $\sim$ December 2009

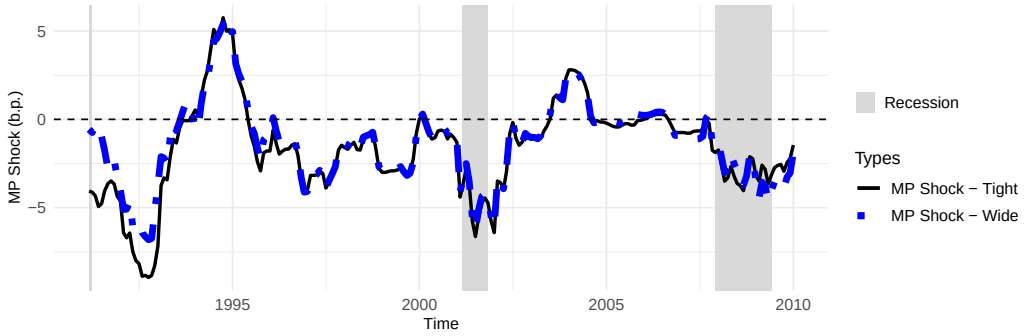

Notes: The monetary policy shocks are obtained by time aggregating high-frequency monetary policy shocks identified from the unexpected jump (drop) in the federal funds rate during 30-minutes (Tight) and one-hour (Wide) windows around the FOMC announcement. To capture the unexpected component in the federal funds rate, I use the change in the rate implied by the current-month federal funds futures contract. All the data on the timings of the FOMC announcement and the high-frequency surprise are from Gurkaynak et al. (2005) and Gorodnichenko and Weber (2016).

E Solution method: the sequence-space global solution method

This section explains the solution method I use to compute the recursive competitive equilibrium. I use the repeated transition method, developed concurrently for the computation of nonlinear aggregate dynamics under aggregate uncertainty in Lee (2025). As highlighted in Bachmann et al. (2013), the strong general equilibrium effect significantly contributes to the linearity in the dynamics of aggregate allocations. However, once the model captures realistic interest-elasticity, the general equilibrium effect is necessarily weakened, leaving the aggregate dynamics highly nonlinear. Due to this highly nonlinear aggregate dynamics in general equilibrium, there are two layers of difficulties in using the algorithm of Krusell and Smith (1998). The first is difficulty in choosing a sufficient statistics for the aggregate dynamics. The model's nonlinear aggregate dynamics might not be sufficiently explained by the moves in aggregate capital stocks, unlike Khan and Thomas (2008). The second difficulty is in setting the parametric form in the law of motion. This problem interacts with the former difficulty because even correctly chosen sufficient statistics would not give accurate computation results due to the wrong specification of the functional form of the law of motion. Therefore, it is almost impossible to jointly identify the correct sufficient statistics and functional form in the law of motion.

The repeated transition method departs from the state-space-based approach, so it does not require a researcher to specify the law of motion. The method exploits the ergodicity of the recursive competitive equilibrium: if a simulated path is long enough, all possible equilibrium allocations should be realized on the path. Then, by simply utilizing the realized allocations including the value functions, the method accurately constructs the rationally expected future value functions at each time on the simulated path.[12]

Using this method, I compute the predicted aggregate allocations, which the time series of the simulated aggregate allocations almost perfectly converges to. And this time series of the predicted aggregate allocations is not based on a parametric form of the law of

[12] As the method relies on the dynamics over the simulated aggregate shock path, it is similar to Boppart et al. (2018). However, the repeated transition method departs from the perfect foresight and is a global solution method.

motion in a state-space representation. Figure E.5 compares the time series of the predicted allocations and the simulated allocations.[13] In the figure, panel (a) shows the predicted aggregate dynamics and the simulated dynamics of the marginal utility, p_t. These two dynamics converged to each other with an extremely small error, as can be seen in the solid line in panel (c). However, if the dynamics of simulated marginal utility are fitted into the log-linear law of motion in the contemporaneous capital stock K_t, the prediction error can become substantially large as in the dashed line in panel (c). A similar pattern is observed in the aggregate dynamics of aggregate capital stock K_t in panel (b). The simulated and predicted paths for K_t are computed at extremely high accuracy with the repeated transition method, while the log-linear fitting leads to a significant prediction error as in panel (d).

Then, I compare the fitness of different specifications of the law of motion by fitting the equilibrium dynamics into each of them.[14] Table E.6 and Table E.7 report the fitness of the different laws of motion of p_t and K_t, respectively. When the law of motion includes only a log of contemporaneous capital stock K_t (specification (1)), the prediction errors remain large, indicating the nonlinear nature of the equilibrium dynamics.[15] However, once the law of motion includes the fragility index in the law of motion (specification (2)), which I define in Section 4.4, the fitness significantly improves for the dynamics of p_t. However, it does not make a significant change in the fitness for the dynamics of K_t. Finally, if the law of motion includes contemporaneous and lagged capital stocks up to three lags in a non-parametric form (specification (3)), the fitness substantially improves from the basic log-linear specification for both p_t and K_t.

[13] This figure is the fundamental accuracy plot suggested in Den Haan (2010).

[14] I compare only the fitness of the law of motion to the converged dynamics of equilibrium allocations. Therefore, if the model is solved based on each of the laws of motion, the implied dynamics might display even greater prediction errors than the reported level.

[15] Den Haan (2010) points out that a slight deviation in R^2 from unity such as $R^2 = 0.995$ can imply a substantially large prediction error and significant nonlinearity.

Figure E.5: Aggregate fluctuations in the marginal utility and the aggregate capital stock

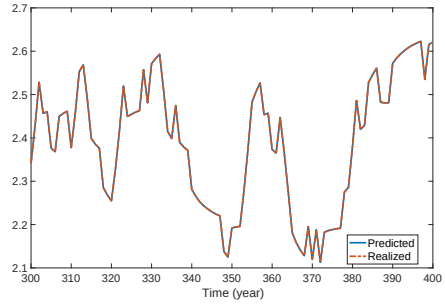

(a) Marginal utility, $p_t = \frac{1}{c_t}$

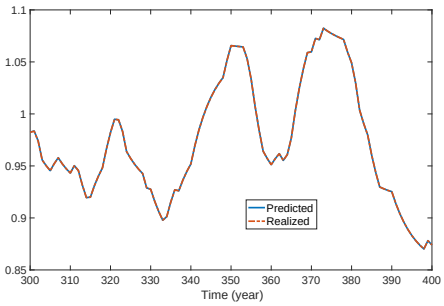

(b) Aggregate capital stock K_t

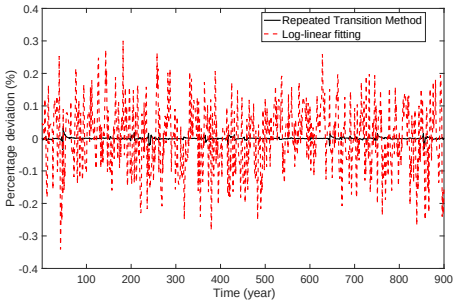

(c) Prediction error in marginal utility

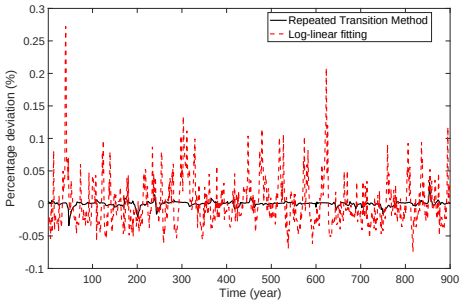

(d) Prediction error in aggregate capital stock

Notes: Panel (a) plots the rationally expected path and the simulated path of the marginal utility. Panel (b) plots the rationally expected path and the simulated path of the aggregate capital stock. Panel (c) plots the prediction errors in the marginal utility path from the repeated transition method and the log-linear fitting. Panel (d) plots the prediction errors in the aggregate capital stock path from the repeated transition method and the log-linear fitting.

Table E.6: The fitness comparison across the different law of motions: p_t

	Dependent variables: $log(p_t)$								
	R^2			$max(\|error\|)(\%)$			$mean(\|error\|)(\%)$		
	(1)	(2)	(3)	(1)	(2)	(3)	(1)	(2)	(3)
A_1	0.9950	0.9989	0.9997	0.1599	0.0903	0.0405	0.0628	0.0251	0.0135
A_2	0.9959	0.9995	0.9999	0.3146	0.1203	0.0685	0.0610	0.0223	0.0098
A_3	0.9957	0.9995	0.9999	0.3160	0.1434	0.0617	0.0661	0.0218	0.0108
A_4	0.9952	0.9994	0.9999	0.3934	0.1091	0.0537	0.0670	0.0234	0.0109
A_5	0.9952	0.9994	0.9999	0.3274	0.1360	0.0546	0.0699	0.0243	0.0117
A_6	0.9957	0.9994	0.9999	0.2560	0.1310	0.0517	0.0639	0.0246	0.0114
A_7	0.9928	0.9991	0.9998	0.1668	0.1030	0.0386	0.0681	0.0179	0.0108

Notes: The table reports R^2, the maximum absolute prediction error, and the mean absolute prediction error by different law of motion (columns) and aggregate states (rows). Specification (1) includes a constant and log of contemporaneous capital stock as a independent variable; Specification (2) includes a constant, log of contemporaneous capital stocks, and log of fragility index as independent variables; Specification (3) includes constant and contemporaneous and lagged capital stocks up to three lags in a non-parametric form as independent variables.

Table E.7: The fitness comparison across the different law of motions: K_{t+1}

	Dependent variables: $log(K_{t+1})$								
	R^2			$max(\|error\|)(\%)$			$mean(\|error\|)(\%)$		
	(1)	(2)	(3)	(1)	(2)	(3)	(1)	(2)	(3)
A_1	1.0000	1.0000	1.0000	0.0651	0.0650	0.0409	0.0117	0.0110	0.0091
A_2	0.9999	0.9999	1.0000	0.1452	0.1454	0.0524	0.0198	0.0200	0.0071
A_3	0.9999	0.9999	1.0000	0.3340	0.3358	0.0445	0.0191	0.0189	0.0072
A_4	0.9999	0.9999	1.0000	0.2455	0.2451	0.0490	0.0211	0.0214	0.0077
A_5	0.9999	0.9999	1.0000	0.2415	0.2412	0.0453	0.0222	0.0221	0.0084
A_6	0.9999	0.9999	1.0000	0.1676	0.1733	0.0473	0.0194	0.0193	0.0085
A_7	0.9998	0.9998	1.0000	0.1275	0.1239	0.0330	0.0168	0.0175	0.0116

Notes: The table reports R^2, the maximum absolute prediction error, and the mean absolute prediction error by different law of motion (columns) and aggregate states (rows). Specification (1) includes a constant and log of contemporaneous capital stock as a independent variable; Specification (2) includes a constant, log of contemporaneous capital stocks, and log of fragility index as independent variables; Specification (3) includes constant and contemporaneous and lagged capital stocks up to three lags in a non-parametric form as independent variables.

F State dependence: further quantification

This section reports extended quantitative results related to the model-side state dependent investment dynamics.

F.1 State dependence - comparison across the models

To quantify how fragility fluctuations drive variation in aggregate investment responses, I exploit the simulated equilibrium path to isolate the role of the endogenous state. Specifically, I identify all periods where the economy experiences a negative one-standard-deviation TFP shock and examine how investment responses vary across different fragility levels. Since the exogenous shock magnitude is held constant across observations, any variation in responses is driven by differences in the endogenous distribution of firms, for which the fragility index serves as a sufficient statistic.[16]

Figure F.6 presents scatter plots of the state-dependent contemporaneous responses of aggregate investment (vertical axis) against the fragility index (horizontal axis) for the baseline model (panel (a)) and a model with convex and constant fixed adjustment costs (panel (b)). The fragility indices are normalized by their standard deviation. The aggregate investment responses are demeaned and expressed as percentage deviations from steady-state levels. To control for variation in TFP levels across episodes, I include fixed effects for each unique combination of prior and contemporaneous TFP states (A_{t-1}, A_t).[17]

Panel (a) reveals a strong negative relationship between the contemporaneous investment response ΔI_t and the fragility index in the baseline model. When fitted to a linear regression:

$$\Delta I_t \text{ (\% w.r.t. s.s. response)} = -7.875 * Fragility_t \ (s.d.) + \epsilon_t, \quad R^2 = 0.677$$
$$(0.173) \tag{1}$$

[16] If there are any responsiveness differences, they are from the endogenous aggregate state, the distribution of firms, as the exogenous states are identical. The fragility index is used as a sufficient statistic for the endogenous aggregate state in this experiment.

[17] The different colors of dots represent the different fixed-effect groups.

Figure F.6: State-dependent responses of aggregate investment

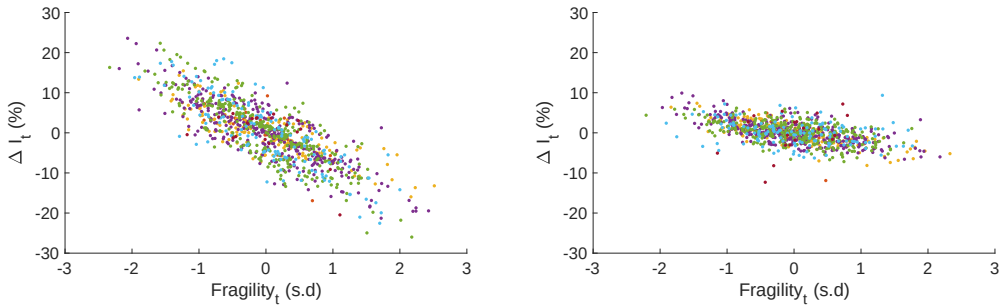

(a) Baseline (b) Constant fixed adj. cost

Notes: The vertical axis of the scatter plot is the instantaneous response of the aggregate investment to a negative one-standard-deviation TFP shock in percentage for baseline model (panel (a)) and a model with convex and constant fixed adjustment costs (panel (b)), and the horizontal axis is the fragility index measured in the unit of standard deviation from the average. In each responses, contemporaneous and one-period-prior aggregate TFP fixed effects are controlled. Using the histogram method in Young (2010), firms are simulated for 5,000 periods (years) based on the recursive competitive equilibrium. The fragility indices are calculated based on the distribution of large firms.

This coefficient implies that a one-standard-deviation increase in fragility amplifies the negative investment response by 7.875% relative to the steady-state response. In contrast, the model with convex and constant fixed adjustment costs (panel (b)) exhibits a significantly weaker relationship (significant at the 1% level), with a coefficient of -2.193. This comparison demonstrates that the baseline model's size-dependent adjustment costs generate substantially stronger endogenous fragility than canonical models.

To assess the output implications of this fragility-driven investment channel, I examine how fragility affects next-period output through the capital accumulation mechanism. When a negative TFP shock coincides with high fragility, the amplified investment decline reduces the future capital stock, resulting in a decline in future output. Following the same identification strategy:

$$\Delta Y_{t+1} \text{ (p.p. w.r.t. s.s.)} = -0.322 * Fragility_t \ (s.d.) + \epsilon_t, \quad R^2 = 0.631$$
$$(0.008) \tag{2}$$

A one-standard-deviation increase in fragility reduces next-period output by 0.322 percentage points through the investment channel. Figure F.7 is a scatter plot of fragility index (horizontal axis) and the aggregate output response (vertical axis), which visualizes the negative relationship.

Figure F.7: State-dependent responses of aggregate output

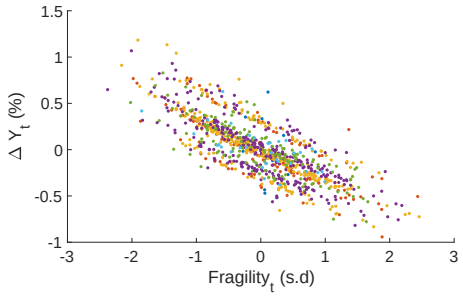

Notes: The vertical axis of the scatter plot is the instantaneous response of the aggregate output to a negative one-standard-deviation TFP shock in percentage point, and the horizontal axis is the fragility index measured in the unit of standard deviation from the average. In each responses, contemporaneous and one-period-prior aggregate TFP fixed effects are controlled. Using the histogram method in Young (2010), firms are simulated for 5,000 periods (years) based on the recursive competitive equilibrium. The fragility indices are calculated based on the distribution of large firms.

The comparison across models (Table G.8) further confirms that the baseline model generates the strongest synchronization patterns and most pronounced aggregate nonlinearities, with all models calibrated to identical targets except for the cross-sectional elasticity ratio.

F.2 State dependence - comparison across the firm size

Having established that fragility generates state-dependent aggregate responses, I now examine which firms drive this effect. Figure F.8 shows the scatter plot of the instantaneous group-level investment responses to a one-standard-deviation negative TFP shock (vertical axis) over the fragility variation in the horizontal axis constructed by large firms (panel (a)) and small firms (panel (b)). As can be seen from the figure, the negative relationship between the responsiveness and the synchronization (fragility) is significantly starker for large firms than for small firms.

Figure F.8: State-dependent responses of investments: large vs. small

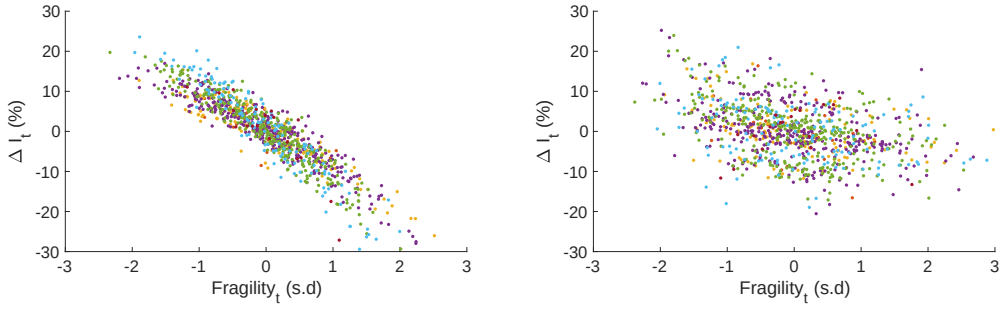

(a) Large firms

(b) Small firms

Notes: The vertical axis of the scatter plot is the instantaneous response of the aggregate investment to a negative one-standard-deviation TFP shock in percentage for large firms (panel (a)) and small firms (panel (b)), and the horizontal axis is the fragility index measured in the unit of standard deviation from the average. In each responses, contemporaneous and one-period-prior aggregate TFP fixed effects are controlled. Using the histogram method in Young (2010), firms are simulated for 5,000 periods (years) based on the recursive competitive equilibrium.

G Synchronization and the aggregate dynamics

Synchronization When an aggregate TFP shock hits, firms accelerate or postpone their investment plans based on their location in the Ss cycle. For example, when a negative aggregate TFP shock hits, firms that are supposed to implement lumpy investments tend to postpone the plan due to the expected underwhelming economic situation. Then, investment timings of these postponing firms and those who plan to invest in the subsequent periods become synchronized. To see this effect, I consider an aggregate negative unexpected TFP shock (MIT shock) to the stationary equilibrium and see how the distribution over the years from the last lumpy investments evolve after the shock. Due to the stochastic nature of the Ss band in the model, there is no deterministic trigger point (small s) in the Ss cycle. However, firms with similar individual states tend to invest at a similar timing after their own last lumpy investments. If it has been a long period since a firm made the last investment, the firm is likely closer to the trigger point, and vice versa. Thus, the years from the last lumpy investments capture the location in the Ss band. To ease the illustration, I will refer to τ as the years from the last lumpy investments.

Figure G.9: Time path of distributions over the Ss band after an MIT shock

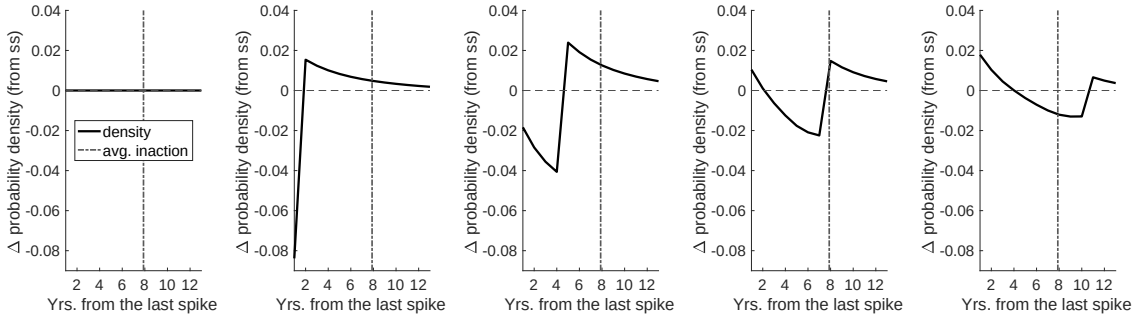

(a) $t = 1$ (b) $t = 2$ (c) $t = 5$ (d) $t = 8$ (e) $t = 11$

Notes: This figure plots the time evolution of the probability density deviations from the stationary equilibrium counterpart after a negative aggregate TFP shock at the stationary equilibrium. Each panel's horizontal axis is for the time (years) from the last lumpy investment, and the vertical axis is for the probability density deviation (a simple difference from the stationary equilibrium's density function).

Figure G.9 plots the time evolution of the large firms' probability mass over the domain of the time from the last lumpy investment, where the vertical axis shows a level deviation

(the difference in the probability mass) from the stationary equilibrium's counterpart. Thus, when the shock hits ($t = 1$, panel (a)), the distribution distance does not deviate from zero, meaning the distribution is the same as in the stationary equilibrium. Due to the expected low marginal profit out of the investment, many firms delay the investment plan leading to a sharp drop in the density for $\tau = 1$ at period $t = 2$ (panel (b)), while the delaying firms contribute to the increase in the probability masses for $\tau > 1$. Then, as time goes by, the synchronized stopping mass is diluted, and in around 8 years, the delayed investment plans tend to form a surge of lumpy investments as can be seen from panel (d) and (e). After around 25 years, the distribution moves back close to the stationary distribution.

Figure G.10: Distributions over the Ss band: large vs. small

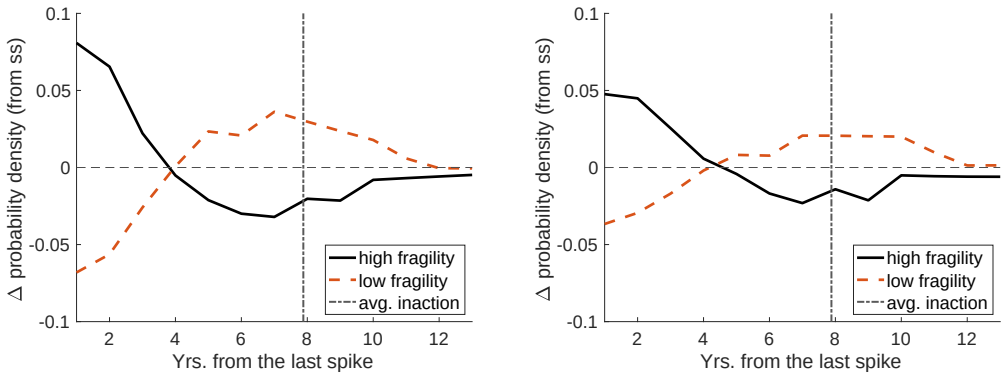

(a) Large firms (b) Small firms

Notes: The solid line is the probability density deviation from the stationary equilibrium counterpart for the highest fragility state in the simulated recursive competitive equilibrium. The dashed line is for the lowest fragility state.

Figure G.10 compares the synchronization pattern between large and small firms for high and low fragility periods. As can be seen from the figure, the distributional difference between the highest and lowest fragility states is starker for large firms than small firms, indicating large firms' stronger synchronization. During the period of highest fragility, a significant portion of large firms have recently completed lumpy investments, indicating that many firms are further away from the trigger point in the Ss band. Specifically, the average time since the last spike is 22% lower than the stationary equilibrium level in high-fragility

periods, while it is 16% higher in low-fragility periods. Small firms display significantly dampened synchronization compared to large firms – in their highest and lowest fragility states, the average years from the last spike are 9.78% lower and 2.65% higher than steady state, respectively.

Aggregate impacts of the synchronization The synchronization patterns documented above have significant aggregate implications. When large firms synchronize their investment timing, this coordination survives general equilibrium forces due to their low interest-rate sensitivity, generating persistent fluctuations in aggregate investment. Figure G.11 plots the impulse responses of the spike ratios (panel (a)) and i_{it}/k_{it} (panel (b)) ratios in different models to a negative one-standard-deviation aggregate TFP shock. The impulse response is computed from the perfect-foresight transition path. The spike ratio is as defined in main text. Each variables' time path is normalized by its volatility (standard deviation) in the simulated path using the global nonlinear solution.

As shown in panel (a), the large firms' spike ratio in the baseline model (solid line) surges after a negative aggregate TFP shock, displaying a synchronization (surge) of the investment timings among large firms. This magnitude of the large firms' synchronization is substantially stronger in the baseline model (solid line) than the model with the linearly size-dependent fixed adjustment cost (dashed line) and the constant fixed adjustment cost (dash-dotted line). On the other hand, the small firms' synchronization (dotted line) is weaker than the large firms' in the baseline model. Similar synchronization patterns are observed in the i_{it}/k_{it} ratios (panel (b)).

This phenomenon happens because a negative aggregate TFP shock triggers a synchronous stop of large-scale investment projects. Then, as the TFP gradually recovers over the transition path, large firms tend to implement large-scale investments at a similar time to the others. If a general equilibrium effect is strong enough, these synchronized lumpy investment timings are supposed to be smoothed. However, the baseline's large firms are inelastic to the general equilibrium effect, so the synchronization survives even in the general equilibrium environment.

Figure G.11: Synchronization after a negative aggregate TFP shock

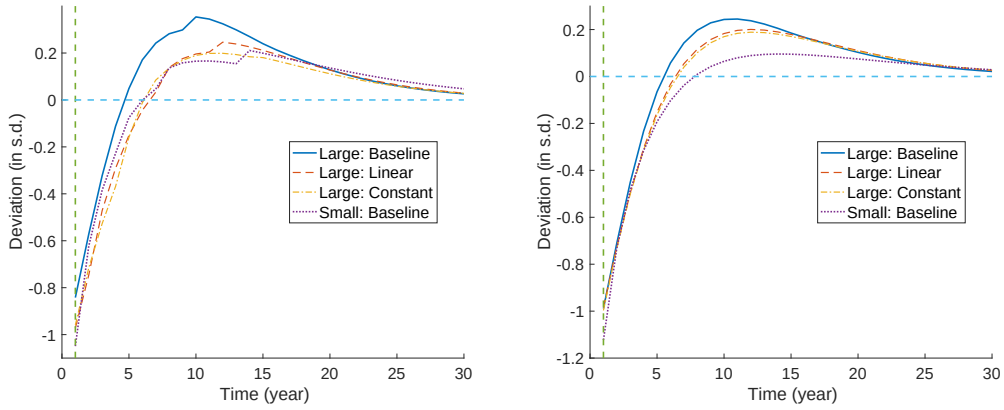

(a) Spike ratio (b) Average i_{it}/k_{it} ratio

Notes: The impulse responses of spike ratio (panel (a)) and average i/k (panel (b)) ratio are obtained from the transition dynamics to the stationary equilibrium allocations after an unexpected negative one-standard-deviation aggregate TFP shock. Each time series is demeaned by the stationary equilibrium levels and normalized by its standard deviation computed from the global solution.

Next, I analyze this synchronization affects the firm and aggregate-level allocations over the business cycle. Table G.8 reports the large firms' synchronization patterns over the business cycle across the models (the first block) and the corresponding high-order moments of the aggregate investment (the second block) and outputs (the bottom block). All the moments are computed based on the global nonlinear solution, which I elaborate on in the following section.

The first two rows report the persistence of the time series of the spike ratio, which is obtained by fitting the series into the $AR(1)$ process. The spike ratio is most persistent in the baseline model, and its persistence decreases as the order of the size dependence in the fixed adjustment cost decreases. Once the general equilibrium effect is lifted by fixing the stochastic discount factor at the steady state (the second row), the persistence ranking is shuffled, and the model with the constant fixed adjustment cost features the strongest persistence. This result shows that the large firms' low sensitivity to the general equilibrium effect in the baseline model is the key to the persistent synchronization. On the other hand, the small firms' persistence of the synchronization is weakest in the baseline model (the

third row).

The following rows in the first block show the high-order moments of the time series of the large firms' spike ratio. The spike ratio displays the largest positive skewness in the baseline model. That is, the large firms tend to be more synchronized in the baseline model than in the others. However, the model with the constant fixed adjustment cost displays the largest skewness in the partial equilibrium. This shows that the low sensitivity to the general equilibrium effect plays a crucial role in synchronizing large firms in the baseline model. For the kurtosis, regardless of the general equilibrium effect, the baseline model features the highest level, while the relative magnitude of the difference is not as substantial as the skewness differences.

Table G.8: Large firms' synchronization and the aggregate dynamics

	baseline ($\zeta = 3.5$)	$\zeta = 2$	$\zeta = 1$	$\zeta = 0$
Large firms' spike ratio				
Persistence - GE	0.769	0.745	0.737	0.735
Persistence - PE	0.751	0.746	0.752	0.762
cf. Small firms' persistence - GE	0.649	0.671	0.690	0.706
Skewness - GE	0.354	0.230	0.195	0.215
Skewness - PE	0.595	0.550	0.586	0.678
Kurtosis - GE	3.235	3.073	2.963	2.935
Kurtosis - PE	5.149	4.947	4.889	4.808
Aggregate investment, $log(I_t)$				
Skewness	-0.124	-0.087	-0.063	-0.055
Kurtosis	2.934	2.904	2.887	2.880
Aggregate output, $log(Y_t)$				
Skewness	-0.017	-0.009	-0.001	0.009
Kurtosis	2.878	2.875	2.875	2.877

Notes: The table reports the firm-level and aggregate-level statistics in the baseline model, the models with quadratically and linearly size-dependent fixed costs, and the model with a constant fixed adjustment cost.

In the following block, I report the high-order moments of the aggregate investment over the business cycle. The aggregate investment displays the most negative skewness and the greatest kurtosis in the baseline model. A similar pattern is observed for the output dynamics reported in the bottom block.

The compared models share the same model structure and are sharply calibrated based on the same target moments except for the cross-section of the elasticity distribution across the large and small firms. Therefore, given the assumption that the target moments are correctly selected, the differences in the high-order moments in the aggregate allocations are driven by the differences in the only unmatched moment: the cross-section of the elasticity distribution. In the following sections, I elaborate further on how the aggregate investment and output become more negatively skewed when the large firms' interest elasticity is as low as the observed level.

H State-dependent interest elasticities of the investment growth in the baseline model

H.1 State-dependent interest rate elasticity of aggregate investment

To study how the aggregate investment responds differently to the same interest shock depending on the fragility state, I hit the economy at each period on the simulated path with an unexpected interest rate shock and compute the contemporaneous response under the partial equilibrium. I compute the elasticity by taking an average of the elasticities from positive and negative 1 % interest rate shocks to account for the asymmetric responses.

Figure H.12: State-dependent semi-elasticities of aggregate investment

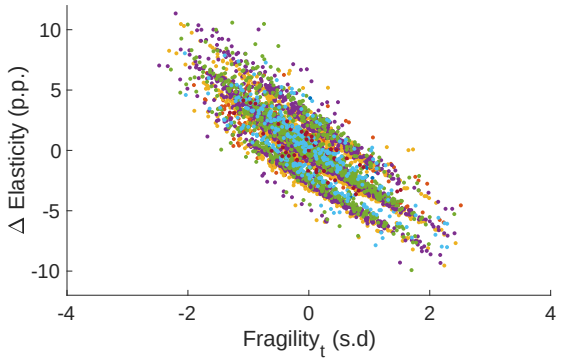

Notes: The vertical axis of the scatter plot is the semi-elasticity of aggregate investment in percentage point deviation from the average, and the horizontal axis is the fragility index in the standard deviation from the average. For each elasticity, contemporaneous and one-period-prior aggregate TFP fixed effects are controlled. Using the histogram method in Young (2010), firms are simulated for 5,000 periods (years) based on the recursive competitive equilibrium. The fragility indices are calculated based on the distribution of large firms.

Figure H.12 is the scatter plot of the interest elasticities of the aggregate investment in relation to the fragility state. The horizontal axis is the fragility index normalized by the standard deviation; the vertical axis is the interest elasticity in percentage deviation from the steady-state level.[18] According to the figure, there is a significant negative relationship between the fragility and the interest elasticity of aggregate investment. By fitting the

[18]The prior and contemporaneous aggregate TFP levels (A_{t-1}, A_t) are controlled by teasing out the pair-specific fixed effect, and the different colors of dots represent the different fixed-effect groups.

relationship into linear regression, I obtain the following result:

$$\Delta Elasticity_t \text{ (\% w.r.t. s.s.)} = -3.350 * Fragility_t \ (s.d) + \epsilon_t, \quad R^2 = 0.689 \qquad (3)$$
$$(0.032)$$

One standard deviation increase in the fragility index decreases the interest elasticity of aggregate investment by around 3.022% compared to the steady-state level. The intuitive explanation for the result is that when the fragility index is high, there are not many large firms that can flexibly participate in and out of large-scale investment. Therefore, the aggregate investments' responsiveness to the interest rate change decreases in a high-fragility state. In Appendix F, I show that the state-dependent elasticity is driven by large firms through the comparison with small firms' effects.

When the fragility index increases by one standard deviation, large firms' investment elasticity decreases by around 5.257%. On the other hand, the same variation in the fragility index decreases small firms' elasticity by 1.244%, and the difference is statistically significant. This result shows that large firms dominantly drive the stark negative relationship between the interest elasticities of the aggregate investments and the fragility index.

H.2 State-dependent elasticity: large vs. small firms

To verify that large firms drive interest elasticity fluctuations in aggregate investment, I compute the elasticity variations separately for large and small firms. Figure H.13 is the scatter plot of interest elasticities along with the fragility variation for large (panel (a)) and small firms (panel (b)). The negative relationship between the fragility index and the elasticity is significantly stronger in large firms. When two different elasticities are fitted into linear regression, the following relationship is obtained:

Figure H.13: State-dependent semi-elasticities of investments: Decomposition

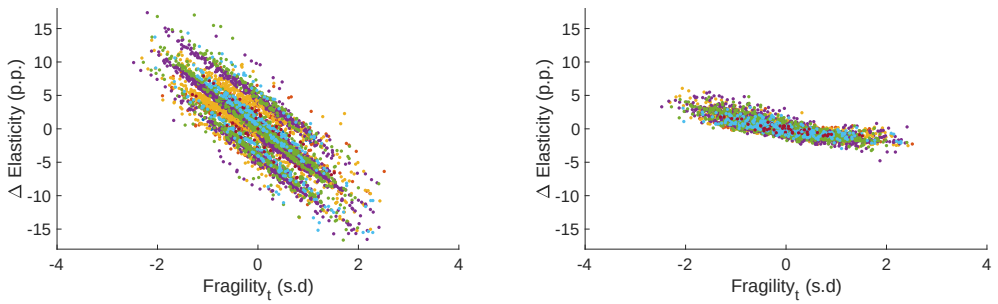

(a) Large firms (b) Small firms

Notes: The vertical axis of the scatter plots is the semi-elasticity of large (panel (a)) and small (panel (b)) firms' investment in percentage point deviation from the average, and the horizontal axis is the fragility index in the standard deviation from the average. For each elasticity, contemporaneous and one-period-prior aggregate TFP fixed effects are controlled. Using the histogram method in Young (2010), firms are simulated for 5,000 periods (years) based on the recursive competitive equilibrium. The fragility indices are calculated based on the distribution of large firms.

$$\Delta Elasticity_t^{Large} \text{ (\% w.r.t. s.s.)} = -5.257 * Fragility_t \ (s.d) + \epsilon_t, \quad R^2 = 0.655 \tag{4}$$

$$(0.054)$$

$$\Delta Elasticity_t^{Small} \text{ (\% w.r.t. s.s.)} = -1.244 * Fragility_t \ (s.d) + \epsilon_t, \quad R^2 = 0.639 \tag{5}$$

$$(0.013)$$

I Additional tables and figures

I.1 Fixed parameters

Table I.9: Fixed Parameters

Parameters	Description	Value
Firm-side Fundamentals		
α	Capital share	0.2800
γ	Labor share	0.6400
δ	Depreciation rate	0.0900
Household		
β	Discount factor	0.9770
TFP Process		
ρ_A	Persistence of aggregate TFP	0.8145

Notes: The fixed parameters are chosen at the level widely used in the relevant literature. The persistence of aggregate TFP is fixed at 0.8145 following Bachmann et al. (2013).

I.2 Predictability for and by the fragility index

Table I.10: Predictability for and by the fragility index

Prediction	for fragility					by fragility	
Dep. var. (*s.d.*):	$Fragility_t$					SR_t	g_t^I
# lags:	$h=5$	$h=4$	$h=3$	$h=2$	$h=1$	$h=0$	$h=0$
SR_{t-h} (*s.d.*)	0.114	0.397	0.753	0.579	0.028		
	(0.166)	(0.118)	(0.081)	(0.137)	(0.176)		
$Fragility_t$ (*s.d.*)						-0.389	-0.464
						(0.216)	(0.260)
Obs.	32	32	32	32	32	32	32
R^2	0.378	0.495	0.806	0.631	0.367	0.371	0.192
Detrend	Yes	Yes	Yes	Yes	Yes	Yes	Yes
Newey-West s.e.	Yes	Yes	Yes	Yes	Yes	Yes	Yes

Notes: This table reports regression results for two exercises: (1) predicting the fragility index using past spike ratios with lags of $h = 1$ to 5 years (columns 1-5), and (2) predicting contemporaneous spike ratio and aggregate investment growth using the fragility index (columns 6-7). All variables are standardized. Dependent variables are detrended using polynomials of time. Newey-West standard errors in parentheses.

I.3 State-dependent sensitivity of the aggregate investment growth

Table I.11: State-dependent sensitivity of the aggregate investment growth: full table

	Dependent variable: $\Delta log(I_t)$ (p.p.)							
	$(-)$ $OutputShock_t$				$(+)$ $OutputShock_t$			
	Model		Data		Model		Data	
	(1)	(2)	(3)	(4)	(5)	(6)	(7)	(8)
$Shock_t$	9.589	9.389	7.193	5.818	8.671	8.490	4.483	6.937
	(0.083)	(0.066)	(1.213)	(1.338)	(0.084)	(0.064)	(1.123)	(1.221)
$Shock_t$		1.537		2.430		-2.011		-1.486
$\times$ $Fragility_t$		(0.042)		(1.311)		(0.045)		(0.495)
Constant	Yes	Yes	Yes	Yes	Yes	Yes	Yes	Yes
Observations	2,296	2,296	16	16	2,706	2,705	18	18
R^2	0.853	0.908	0.730	0.790	0.730	0.884	0.515	0.705
Adjusted R^2	0.853	0.908	0.709	0.755	0.709	0.884	0.483	0.663

Notes: The dependent variable is the growth rate of aggregate investment. The independent variables are output shocks obtained from fitting output series into an AR(1) process and the interaction between the output shock and the fragility index. The fragility index is based on the years since the last lumpy investment of large firms. The first two columns report the regression coefficients from the simulated data when the negative output shock hits. The third and fourth columns report the regression coefficients using Compustat data when the negative output shock hits. The fifth and sixth columns report the regression coefficients from the simulated data when the positive output shock hits. The last two columns report the regression coefficients using Compustat data when the positive output shock hits. The numbers in the brackets are standard errors.

I.4 Business cycle statistics

Table I.12: Business cycle statistics

	Data	Model
$corr(Y_t, Y_{t-1})$	0.941	0.847
$corr(I_t, I_{t-1})$	0.742	0.740
$corr(C_t, C_{t-1})$	0.954	0.907
$corr(I_t, Y_t)$	0.795	0.796
$corr(L_t, Y_t)$	0.898	0.763
$corr(C_t, Y_t)$	0.978	0.981
$sd(Y_t)$	0.060	0.067
$sd(I_t)/sd(Y_t)$	1.976	1.767
$sd(C_t)/sd(Y_t)$	0.945	0.829

Notes: The business cycle statistics are obtained from the simulated data using the dynamic stochastic general equilibrium allocations. All the variables are in log and linearly detrended. The data counterpart is from National Income and Product Accounts (NIPA) data.

I.5 Firm-level supporting evidence for the state dependence

This section reports firm-level evidence that large firms' responsiveness to monetary policy shocks becomes insignificant during high fragility periods. The regression setup follows Table 2, where the first column reports results for high fragility periods and the second for low fragility periods. High and low fragility periods are defined as the top 40% and bottom 40% of fragility index values in the sample.

The results show that large firms' extensive-margin response to monetary policy is statistically insignificant during high fragility periods (-0.646 with the standard error of 0.547), while it remains significant at the 10% level during low fragility periods (-0.945 with the standard error of 0.543). This loss of statistical significance during high fragility periods supports the model's prediction that synchronized large firms become unresponsive to interest rate changes when many are far from their investment triggers.

Table I.13: State-dependent extensive-margin investment sensitivities to the MP shocks

	Dependent variable: $\mathbb{I}\{\frac{I_{it}}{k_{it}} > 0.2\}$	
	High fragility	Low fragility
MP_t	-0.646	-0.945
	(0.547)	(0.543)
Obs.	15,963	13,434
R^2	0.664	0.695
Firm FE	Yes	Yes
Sect.-year FE	Yes	Yes
Firm-level ctrl.	Yes	Yes
Two-way cl.	Yes	Yes

Notes: The independent variables include monetary policy shocks, fixed effects (firm and sector-year), and firm-level control variables (lagged current account (ACT_{t-1}), lagged total debt (DT_{t-1}), and operating profit ($OIBDP_t$) normalized by lagged total asset (AT_{t-1}), log of lagged capital stock, and log of employment (EMP_t)). The numbers in the bracket are the standard errors. The standard errors are clustered two-way by firm and year.

J Notes on the recursive competitive equilibrium

J.1 Value function normalization

I multiply $p(S) = 1/C(S)$ on the both sides of line (16) to obtain

$$p(S)J(k,z;S) = \quad p(S)(\pi(k,z;S) + (1-\delta)k) \tag{6}$$

$$+ \int_0^{\bar{\xi}} \max\left\{p(S)R^*(k,z;S) - p(S)w(S)F(k,\xi), p(S)R^c(k,z;S)\right\} dG_\xi(\xi) \tag{7}$$

I define the normalized value functions as follows:

$$\widetilde{J}(k,z;S) := p(S)J(k,z;S) \tag{8}$$

$$\widetilde{R}^*(k,z;S) := p(S)R^*(k,z;S) \tag{9}$$

$$\widetilde{R}^c(k,z;S) := p(S)R^c(k,z;S) \tag{10}$$

It is necessary to check whether the recursive formulation naturally follows for the normalized value functions. Using $p(S)q(S,S') = \beta p(S')$,

$$\widetilde{R}^* = \max_{k' \geq 0} \ (-k' - c(k,k'))p(S) + \mathbb{E}p(S)q(S,S')J(k',z';S') \tag{11}$$

$$= \max_{k' \geq 0} \ (-k' - c(k,k'))p(S) + \mathbb{E}\beta p(S')J(k',z';S') \tag{12}$$

$$= \max_{k' \geq 0} \ (-k' - c(k,k'))p(S) + \beta\mathbb{E}\widetilde{J}(k',z';S') \tag{13}$$

Similarly,

$$\widetilde{R}^c = \max_{k^c \in \Omega(k)} \ (-k^c - c(k,k^c))p(S) + \beta\mathbb{E}\widetilde{J}(k^c,z';S'). \tag{14}$$

Therefore, the recursive form is preserved for the normalized value functions. As in Khan and Thomas (2008), the recursive form based on the normalized value function eases computation of the dynamic stochastic general equilibrium because the price, p, depends only

on the current aggregate state variable, S.

J.2 Recursive competitive equilibrium

In this section, I define the recursive competitive equilibrium in the economy.
$(g_c, g_a, g_{l_H}, g_{k^*}, g_{k^c}, g_{\xi^*}, g_l, \widetilde{V}, \widetilde{J}, \widetilde{R}^*, \widetilde{R}^c, p, w, G, H)$ is a recursive competitive equilibrium if the following conditions are satisfied.

1. $g_c, g_{lH}, \widetilde{V}$, and g_a, solve the household's problem.
2. $g_{k^*}, g_{k^c}, g_{\xi^*}, g_l, \widetilde{J}, \widetilde{R}^*$, and $\widetilde{R}^c$ solve a firm's problem.
3. Market Clearing:

$$\text{(Labor Market)} \qquad g_{lH}(\Phi; S) = \int \Bigg(g_l(k, z; S) + \left(\frac{g_{\xi^*}(k, z; S)}{\overline{\xi}}\right)\left(\frac{g_{\xi^*}(k, z; S)}{2}\right) k^{\zeta} \Bigg) d\Phi$$

$$\begin{aligned} \text{(Product Market)} \qquad g_c(\Phi; S) = \int \Bigg(& zAk^{\alpha} g_{n_d}(k, z; S)^{\gamma} \\ & - \Big((g_{k^*}(k, z; S) - (1-\delta)k) + c(k, g_{k^*}(k, z; S)) \Big) \\ & \times \frac{g_{\xi^*}(k, z; S)}{\overline{\xi}} \\ & - \Big((g_{k^c}(k, z; S) - (1-\delta)k) + c(k, g_{k^c}(k, z; S)) \Big) \\ & \times \frac{1 - g_{\xi^*}(k, z; S)}{\overline{\xi}} \Bigg) d\Phi \end{aligned}$$

4. Consistency Condition:[19]

$$\begin{aligned} \text{(Consistency)} \quad & G_{\Phi}(\Phi) = H(\Phi) = \Phi', \text{ where for } \forall K' \subseteq \mathbb{K} \text{ and } z' \in \mathbb{Z}, \\ & \Phi'(K', z') = \int \Gamma_{z,z'} \Bigg(\mathbb{I}\{g_{k^*}(k, z; S) \in K'\} \frac{g_{\xi^*}(k, z; S)}{\overline{\xi}} \\ & \qquad + \mathbb{I}\{g_{k^c}(k, z; S) \in K'\} \frac{1 - g_{\xi^*}(k, z; S)}{\overline{\xi}} \Bigg) d\Phi \end{aligned}$$

[19] $\mathbb{K}$ and $\mathbb{Z}$ are the supports of the marginal distributions of capital and productivity induced from Φ.

K Robustness check and comparative statics

In this section, I check the robustness of the key empirical and theoretical results. Sections K.1 and K.2 replicate the empirical analysis with spike cutoffs at 18% and 22% instead of the baseline 20%. Specifically, Figure 1 and Figure 2 in the main text, as well as Figure A.1 and Table I.10 in the Appendix, are replicated with these alternative thresholds. All results remain robust across different thresholds, and the fragility index's predictive power for contemporaneous investment variables becomes even weakly stronger with the 18% threshold.

Section K.3 examines how the state-dependent investment response varies with the size-dependence parameter ζ. Table B.2 shows that different ζ values generate different cross-sectional interest elasticity patterns. The state dependence exhibits a monotonic relationship with ζ: higher values strengthen the fragility mechanism. For example, $\zeta = 3.7$ produces results similar to the baseline $\zeta = 3.5$, while lower values like $\zeta = 0$ substantially weaken the state-dependent response, confirming that the mechanism requires sufficient size dependence to operate.

K.1 Robustness check: spike thresholds at 18%

Figure K.14: Three surges of large firms' lumpy investments before recessions

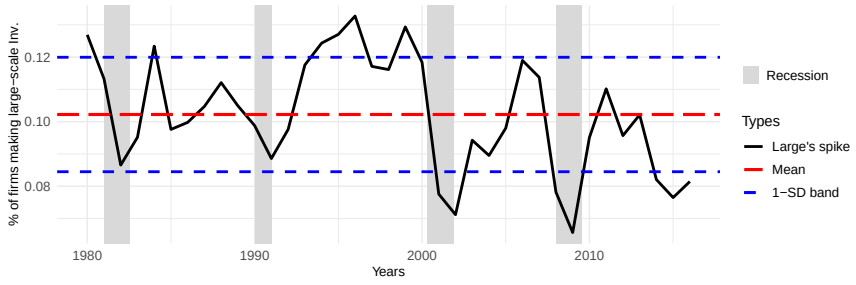

Notes: The firm-level large-scale investment is defined as an investment greater than 20% of the existing capital stock. The solid line plots the time series of the fraction of large firms making large-scale investments. The grey areas indicate the NBER recession periods.

Figure K.15: Conditional heteroskedasticity of aggregate investment

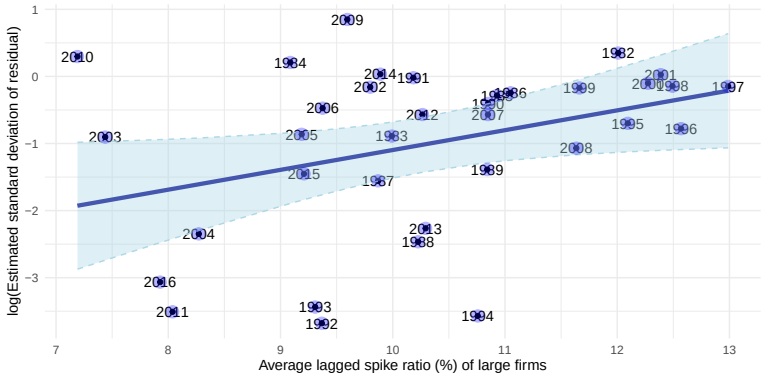

Notes: The estimated standard deviation of the residual (y-axis) is obtained from fitting the aggregate investment-to-capital ratio (%) into an autoregressive process with four lags. The average lagged spike ratio of large firms (%) is obtained by averaging the most recent past two spike ratios for each observation of residualized investments. The years overlaid on the dots are the observed years of the residualized investment-to-capital ratios.

Figure K.16: Fragility, spike ratio, and the aggregate investments

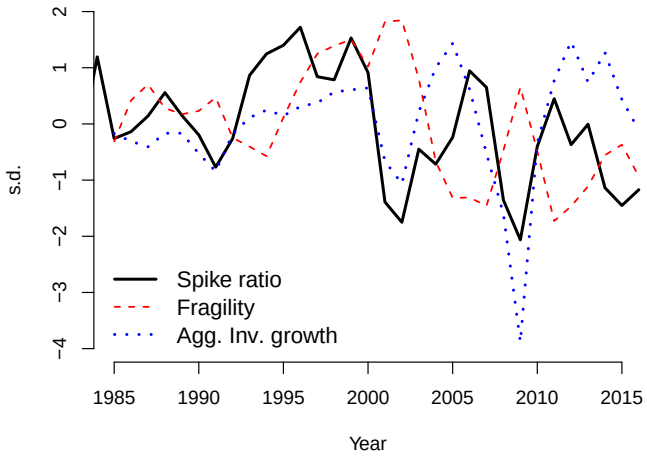

Notes: The solid line plots the time series of the spike ratio. The dashed line is the time series of the fragility index. The dotted line is time series of the aggregate investment growth rate.

Table K.14: Predictability for and by the fragility index

Prediction	for fragility					by fragility	
Dep. var. (*s.d.*):	$Fragility_t$					SR_t	g_t^I
# lags:	$h=5$	$h=4$	$h=3$	$h=2$	$h=1$	$h=0$	$h=0$
SR_{t-h} (*s.d.*)	0.153	0.442	0.782	0.536	0.079		
	(0.166)	(0.119)	(0.091)	(0.148)	(0.177)		
$Fragility_t$ (*s.d.*)						-0.485	-0.467
						(0.196)	(0.249)
Obs.	32	32	32	32	32	32	32
R^2	0.363	0.501	0.809	0.566	0.348	0.438	0.199
Detrend	Yes	Yes	Yes	Yes	Yes	Yes	Yes
Newey-West s.e.	Yes	Yes	Yes	Yes	Yes	Yes	Yes

Notes: This table reports regression results for two exercises: (1) predicting the fragility index using past spike ratios with lags of $h = 1$ to 5 years (columns 1-5), and (2) predicting contemporaneous spike ratio and aggregate investment growth using the fragility index (columns 6-7). All variables are standardized. Dependent variables are detrended using polynomials of time. Newey-West standard errors in parentheses.

K.2 Robustness check: spike thresholds at 22%

Figure K.17: Three surges of large firms' lumpy investments before recessions

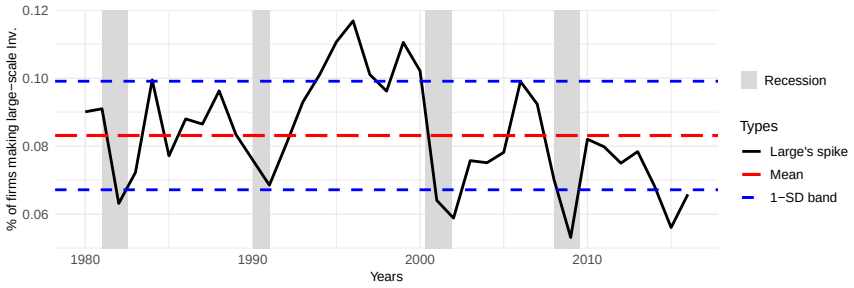

Notes: The firm-level large-scale investment is defined as an investment greater than 20% of the existing capital stock. The solid line plots the time series of the fraction of large firms making large-scale investments. The grey areas indicate the NBER recession periods.

Figure K.18: Conditional heteroskedasticity of aggregate investment

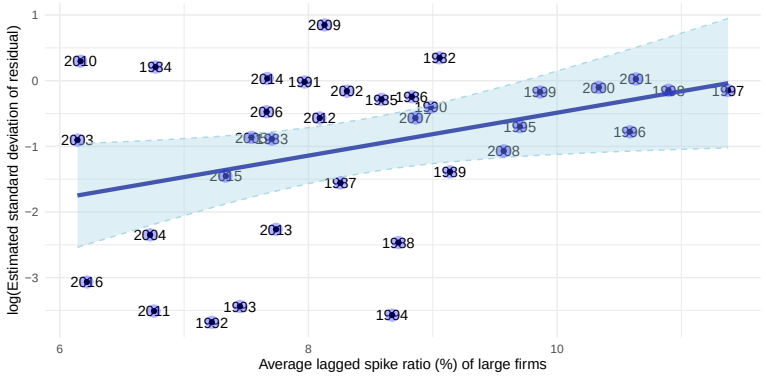

Notes: The estimated standard deviation of the residual (y-axis) is obtained from fitting the aggregate investment-to-capital ratio (%) into an autoregressive process with four lags. The average lagged spike ratio of large firms (%) is obtained by averaging the most recent past two spike ratios for each observation of residualized investments. The years overlaid on the dots are the observed years of the residualized investment-to-capital ratios.

Figure K.19: Fragility, spike ratio, and the aggregate investments

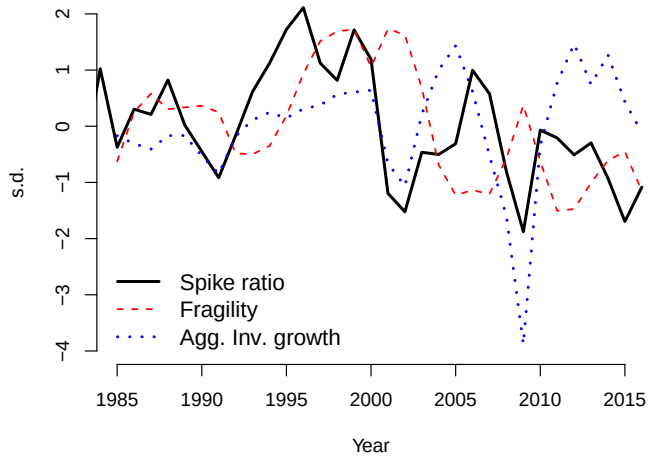

Notes: The solid line plots the time series of the spike ratio. The dashed line is the time series of the fragility index. The dotted line is time series of the aggregate investment growth rate.

Table K.15: Predictability for and by the fragility index

Prediction	for fragility					by fragility	
Dep. var. (*s.d.*):	$Fragility_t$					SR_t	g_t^I
# lags:	$h=5$	$h=4$	$h=3$	$h=2$	$h=1$	$h=0$	$h=0$
SR_{t-h} (*s.d.*)	0.114	0.368	0.736	0.616	0.137		
	(0.162)	(0.119)	(0.072)	(0.134)	(0.178)		
$Fragility_t$ (*s.d.*)						-0.235	-0.386
						(0.228)	(0.249)
Obs.	32	32	32	32	32	32	32
R^2	0.418	0.516	0.816	0.691	0.356	0.371	0.144
Detrend	Yes	Yes	Yes	Yes	Yes	Yes	Yes
Newey-West s.e.	Yes	Yes	Yes	Yes	Yes	Yes	Yes

Notes: This table reports regression results for two exercises: (1) predicting the fragility index using past spike ratios with lags of $h = 1$ to 5 years (columns 1-5), and (2) predicting contemporaneous spike ratio and aggregate investment growth using the fragility index (columns 6-7). All variables are standardized. Dependent variables are detrended using polynomials of time. Newey-West standard errors in parentheses.

K.3 Sensitivity check: size curvature parameter in the fixed cost

Figure K.20: Semi-elasticities of investments across different calibrations

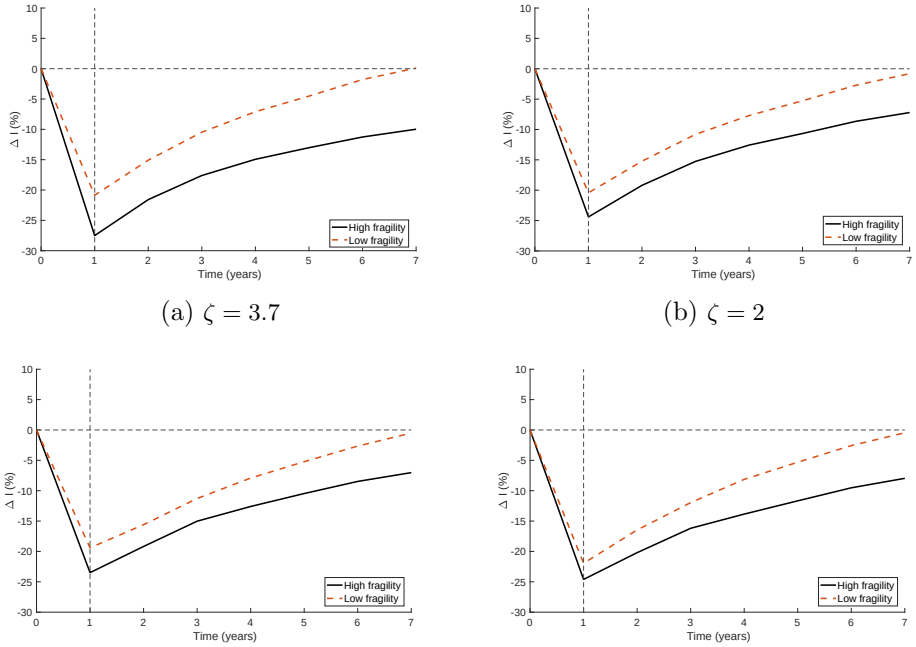

(a) $\zeta = 3.7$ (b) $\zeta = 2$

(c) $\zeta = 1$ (d) $\zeta = 0$

Notes: The solid line is the impulse response to the TFP shock when the fragility index is two standard deviations above the stationary equilibrium level. The dashed line is for the state where the fragility index is two standard deviations below the stationary equilibrium.

References

Autor, D., D. Dorn, L. F. Katz, C. Patterson, and J. Van Reenen (2020). The Fall of the Labor Share and the Rise of Superstar Firms. *The Quarterly Journal of Economics*.

Bachmann, R., R. J. Caballero, and E. M. R. A. Engel (2013, October). Aggregate Implications of Lumpy Investment: New Evidence and a DSGE Model. *American Economic Journal: Macroeconomics 5*(4), 29–67.

Boppart, T., P. Krusell, and K. Mitman (2018, April). Exploiting MIT shocks in heterogeneous-agent economies: the impulse response as a numerical derivative. *Journal of Economic Dynamics and Control 89*, 68–92.

Den Haan, W. J. (2010, January). Assessing the accuracy of the aggregate law of motion in models with heterogeneous agents. *Journal of Economic Dynamics and Control 34*(1), 79–99.

Fernald, J. (2014). A Quarterly, Utilization-Adjusted Series on Total Factor Productivity. *Federal Reserve Bank of San Francisco, Working Paper Series*, 01–28.

Gorodnichenko, Y. and M. Weber (2016, January). Are Sticky Prices Costly? Evidence from the Stock Market. *American Economic Review 106*(1), 165–199.

Gurkaynak, R. S., B. Sack, and E. T. Swanson (2005). Do Actions Speak Louder Than Words? The Response of Asset Prices to Monetary Policy Actions and Statements. *International Journal of Central Banking 1*(1), 39.

Jeenas, P. (2018). Monetary Policy Shocks, Financial Structure, and Firm Activity: A Panel Approach. *SSRN Electronic Journal*.

Khan, A. and J. K. Thomas (2008, March). Idiosyncratic Shocks and the Role of Nonconvexities in Plant and Aggregate Investment Dynamics. *Econometrica 76*(2), 395–436.

Koby, Y. and C. K. Wolf (2020). Aggregation in Heterogeneous-Firm Models: Theory and Measurement. *Working Paper*, 66.

Krusell, P. and A. Smith, Jr. (1998, October). Income and Wealth Heterogeneity in the Macroeconomy. *Journal of Political Economy 106*(5), 867–896.

Lee, H. (2025). Global Nonlinear Solutions in Sequence Space and the Generalized Transition Function. *Working paper*.

Ottonello, P. and T. Winberry (2020). Financial Heterogeneity and the Investment Channel of Monetary Policy. *Econometrica 88*(6), 2473–2502.

Winberry, T. (2021, January). Lumpy Investment, Business Cycles, and Stimulus Policy. *American Economic Review 111*(1), 364–396.

Young, E. R. (2010, January). Solving the incomplete markets model with aggregate uncertainty using the Krusell–Smith algorithm and non-stochastic simulations. *Journal of Economic Dynamics and Control 34*(1), 36–41.

Zwick, E. and J. Mahon (2017, January). Tax Policy and Heterogeneous Investment Behavior. *American Economic Review 107*(1), 217–248.